

CHAPTER 2 LITERATURE REVIEW

The purpose of this chapter is to review the literature. The review of literature is divided into 4 parts: AE sensor, calibration systems of AE sensor, internal valve leakage rate measurement using AE and corrosion monitoring using AE. In the first part, the design of AE sensors, PZT materials and backing materials are reviewed. In the second part, the calibration systems of AE sensor, traceability of AE measurement systems and the method for analysis the output voltage of AE sensor are reviewed. In the third and last parts, the internal valve leakage rate measurement and the corrosion monitoring using AE are reviewed, respectively.

2.1 AE Sensor

Hill and El-dardiry (1981) reported the variables in the use and design of AE sensors. The variable is the acoustic impedance or layered medium. The AE sensor is a layered medium. The medium 1 is usually steel or some other metal. The medium 2 is the coupling layer, which may be grease, oil or a solid. The medium 3 will be wear plate that is usually present. The medium 4 is the PZT material that carries out the acousto-electric transduction process. The medium 5 may be air or backing material. The theory is derived for describe the acoustic impedance of each layer. The couplant gauge is used to measure the couplant thickness. The ultrasonic transducer is used to generate the AE source for proof the mathematical modeling. The result shows that the agreement between theory and experiment is quite good. This means that the theory provides a basic for a better understanding of the effect of couplant thickness on measured AE parameters.

Fortunko et al. (1992) presented the modeling and experiments of high reliability of AE sensors. A computer model is used to evaluate the suitability of five PZT materials for use in broadband (10 kHz – 2 MHz) AE point sensors. The computer model is accounted for the effects of the electrical loading of the PZT material by the input impedance of the preamplifier and the mechanical loading by the specimen and backing materials. The authors are compared the model predictions with results of measurements, which are normalized using the NISI Standard Reference Material (SRM) conical transducer. The effect of selecting different PZT materials (PZT-5A, Lead Metaniobate, X-cut Quarts, 36° Y-cut LiNbO₃, and PVDF) and transducer configurations (“pinducer” vs. “conical”) are evaluated experimentally and analytically. The results show that materials exhibiting the highest dielectric constant, ϵ_{33}^s , are best suited for high performance AE sensor applications. In addition, it is concluded that field-effect transistors exhibiting very small noise currents, less than $1.9 \text{ fA}/\sqrt{\text{Hz}}$, are required to maximize the low frequency signal to noise performance of PZT-5A sensors.

Holroyd and Matlock (1995) presented the resonant AE sensor (invention). An AE sensor consists of a resonant detection element (cylindrical shape having electrodes on its end faces) that is attached to the base-plate by a small area in comparison to the overall surface area of the resonant detection element. The base-plate is of a multi-layer construction including an insulating layer onto that an electrically conducting circuit is formed. The area of attachment is positioned with respect to the wave motion during the resonance of the resonant detection element. This effect is not significant effect on the resonant detection element. The elastic waves from the base-plate to the resonant

detection element at the desired frequency are introduced. The damping material for reproducible characteristics of resonant frequency and rate of damping is fabricated from silicone rubber.

Sugishita and Ku (1997) presented the multiple elements PZT sensor (invention). A PZT sensor has groups of a first part and second part there between. Thin PZT ceramic layers in groups and thick PZT ceramic layers in the second part are polarized in the direction of thickness. All of electrodes are layers, and each electrode is provided between the PZT ceramic layers. A step-up output voltage is generated between the PZT ceramic layers of the second part by longitudinal vibration of the PZT ceramic layers of the groups. The output voltage of the multiple elements PZT sensor is higher than the single element PZT sensor.

Don et al. (1999) presented the sensor backing material and method of application. The backing materials are fabricated from a plurality of tungsten powder associated with epoxy resin, and a plurality of silver powder associated with epoxy resin. The mixtures are mixed in the mold at an atmospheric pressure. The backing material is cured during manufacture at a pressure of approximately 101 kPa. The acoustic impedance of both backing materials is approximately $7.5 \text{ kg/m}^2\text{s} \times 10^6$. The housing supporting the epoxy resin backing material is electrically conductive and connected to at least one electrically conductive lead.

Tantawy and Sung (2003) presented a new composite material fabricated from porous epoxy resin containing titanium (Ti), silane coupling agent and plasticizer composites for ultrasonic attenuation backing. The macromolecular network of epoxy resin is modified considerably by the inclusion of Ti powder, coupling agent and plasticizer as confirmed by network structure and mechanical analyzes. The ultrasonic parameters in epoxy composites are measured by a conventional pulse-echo-overlap technique at a frequency of 1-5 MHz. The effect of Ti content and temperature on the longitudinal sound velocity and attenuation of epoxy resin composites are investigated. From the results, the ultrasonic sound velocity and the attenuation decrease with raising temperature due to the dilatation effect of the epoxy matrix. The attenuation increases with increasing Ti content and frequency in porous epoxy composites. The acoustic impedance also increases with increasing Ti content. The high attenuation and acoustic impedance values reflect that the porous epoxy-Ti composites are useful for transducer backing applications.

Callens et al. (2004) proposed a simple matching device using two matching layers where one of them is made of glue (the acoustic impedance between a PZT sensor and a water load). The characteristic acoustic impedance of the PZT is around $33 \text{ kg/m}^2\text{s} \times 10^6$. Theoretically, a quarter-wave layer with characteristic acoustic impedance equal to $7 \text{ kg/m}^2\text{s} \times 10^6$ is necessary to match the sensor to water. In practice, it is difficult to find a material with this particular impedance. In this study, the thicknesses are not equal to a quarter of the individual wave length. The first and second matching layers are made from the glass and glue, respectively. The thickness of each matching layer is then calculated as a function of the characteristic acoustic impedance of the two layers. The influence of the thickness of these layers is discussed. Finally, a specific specimen is presented and the transmission coefficient is measured. The experimental and analytical results are in good agreement, which validates the proposed technique.

Lee and Lin (2006) reported a new type miniature piezoelectric conical sensor for AE measurements. The aim of authors is to present the fabrication, construction, and experimental testing of a new type of miniature-conical sensor for AE measurements. Excimer lasermicro-machining technique is introduced in this study for fabricating the miniature-conical PZT elements. A compact design in constructing the mini-conical sensor using the miniature PZT elements is proposed and tested. Conical PZT elements with contact size less than $300\ \mu\text{m}$ are constructed. Standard AE testing on a polymethyl methacrylate (PMMA) plate using glass capillary breaking are performed to evaluate the performance of the constructed miniature conical sensor. Good experimental data are observed that can match the theoretical counterparts. From the results, the sensors can be very useful in many applications involving quantitative measurements of transient elastic waves.

Kirk et al. (2007) presented the high-temperature-resistant PZT sensor used as AE sensor over a temperature range from room temperature up to 400°C . The PZT-composites consisted of lithium niobate pillars in a cement matrix with a lithium niobate volume fraction of 45%. Two different crystal orientations of lithium niobate and two different thicknesses, 2 mm and 4 mm, are tested. Three sensors are compared at the room temperature. The results show that all sensors are able to detect the simulated AE signal. In addition, satisfactory room temperature operation of the sensors is verified by measurements of AE source location using two signals detected by two devices at different distances from the source. The high-temperature tests show that all three PZT-composites are easily able to detect AE signals up to 400°C . However, there is some variation in sensitivity with temperature that may be due to couplant effects and should be further investigated.

Cunfu et al. (2007) presented the design of a PZT sensor cylindrical phase modulator for simulating AE signals in pipe leak. On the basis of the PZT equations and electromechanical equivalence principle, the transfer function of a PZT cylindrical phase modulator is delivered. A PZT cylindrical phase modulator is designed, and the numerical simulation is run using LabVIEW software. The results of number simulation verify that the designed phase modulator can simulate effectively simulate leak AE signals when the frequency is less than 25 kHz. Thus, the phase modulator can be used to conduct research on the optical fiber sensing technology for pipeline leak detection in the laboratory.

Kazys et al. (2008) reviewed the PZT material and bonding method of high temperature ultrasonic sensors. More than 10 PZT materials suitable for operation at high temperatures are overviewed. From the reviewed results, for operation at high temperature the most suitable are PZT elements made of the following materials: bismuth titanate $\text{Bi}_4\text{Ti}_3\text{O}_{12}$ (BIT); modified BIT; lead metaniobate; BIT/PZT film. For bonding of the PZT elements to the protector the thermo-sonic gold-to-gold or silver-to-silver diffusion bonding method may be proposed. This process must be still optimized. In the BIT/PZT film approach the bonding procedure is avoided at all. Design of high temperature ultrasonic sensors depends on the PZT element and the bonding method selected. The sensor may be direct contact type, placed into Inconel-600 or stainless steel housing, with a thicker protector, thus the backing material may not be necessary (protector damps the PZT element). Electrical connection with the sensor is provided by a high temperature metallic cable, which is by a laser welded to the housing. Electrical connection of the PZT element to the cable and other inner connections may be

provided by means of the soldered or with gold-to-gold bonded or pressed gold wires or foil strips.

Hong et al. (2008) studied the characteristics of AE sensor using lead-free (LiNaK)-(NaTaSb)O₃ ceramics for fluid leak detection in power plant valves. In this study, AE sensor is fabricated using lead-free (LiNaK)-(NbTaSb)O₃ ceramics for preventing environmental pollution. The structure of the AE sensor is designed as a Langevin-type one with air backing. The electromechanical coupling factor (k_p) and piezoelectric constants d_{33} and g_{33} of lead-free (LiNaK)-(NbTaSb)O₃ ceramics are 0.49, 300 $\rho C/N$, 27.02 mV·m/N, respectively. The peak sensitivity and frequency of the AE sensor using this ceramic material are 66.3 dB and 29.4 kHz, respectively. From the results, the characteristics of AE sensor using lead-free ceramics for fluid leak detection in power plant valves show that the peak frequency of response is 25 kHz at 2 and 6 kgf/cm² N₂ gas pressures, and increased up to 50 kHz at a 10 kgf/cm² N₂ gas pressure. The magnitude of the response voltage is about 40 mV at all the pressures.

State et al. (2010) developed and analyzed the ultrasound backing materials based on polymer composites with improved dimensional stability and low coefficient of thermal expansion. For this study, a filled epoxy resin (Stycast₁₂₆₅), a commonly used backing material, is considered reference material and polyurethane composites (PU₂₃₀₅, PU₂₃₅₀) are proposed as better alternatives. When compared to the reference, the PU₂₃₅₀ filled with a mixture of Al₂O₃ and tungsten exhibited an approximately 15 times lower glassy transition temperature and a 2.5 time lower longitudinal thermal expansion at 20° C. This ensures that within the entire operational temperature range the backing material is flexible, minimizing the thermal stresses induced onto sensor elements soldered joints and PZT core. From the results, the attenuation at 5 MHz is similar to the reference material while at 7 and 8.5 MHz it is 33 % and 54 % higher respectively for the same material. It is concluded that the newly developed polyurethane composites outperform the reference backing with respect to the thermal dimensional stability as well as to the damping properties. An integrated rigorous mechano-acoustical approach is being proposed as an appropriate passive material design path. It can be easily extended to any other passive materials used for ultrasound sensor conception.

2.2 Calibration of AE Sensor

In order to calibrate a sensor absolutely, the mechanical input to the sensor must be known or be calculable to a high degree of accuracy. The electrical output from the sensor can then be compared with the known mechanical input and the absolute frequency response of the sensor/amplifier system calculated. The literature review of AE sensor calibration is reviewed. The details are shown below.

2.2.1 Primary Calibration

Keprt and Benes (2007) reviewed the background, the methodology and the standardization of the primary calibration of AE sensors and studied the determination of uncertainty in calibration of AE sensors. The method of reciprocity calibration and the step function calibration are described and explained. A transfer medium for wave propagation a large steel block (a cylindrical steel block 0.9 m in diameter 0.43 m long with optically polished end faces) is used to study. The method of step function calibration is described in ASTM E 1106. For the method of reciprocity calibration, the software and measuring apparatus enables primary calibration of AE sensors according

to NDIS 2109. The comparison of the results of the both method show that the shape corresponds well, but there is a difference in amplitude. The higher curve is from reciprocity calibration. The reason for difference is that the signal from capillary break is calculated and is different from real signal. The uncertainty of measurement by reciprocity calibration in range from 60 kHz to 285 kHz is ± 3 dB and from 285 kHz to 1 MHz is up to ± 8 dB. The big influence on uncertainty in reciprocity calibration is the influence of remounting reference sensor and pair sensors. This influence is possible to suppress by correct and precise mounting of the sensors. The repeatability in the step function calibration is in general worse than in reciprocity calibration (Keprt and Benes, 2008).

2.2.2 Air Jet System Calibration

Green (1978) described and presented a low cost method for the measurement of absolute signal of AE sensor systems by a jet of helium gas induced AE energy source. Two AE sensor are examined, a wideband and a resonant (140 kHz) sensors. The 100 mm long, 115 mm diameter aluminium block is used. The parameters of helium jet are 0.8 mm of jet bore diameter, 3.0 mm of jet stand-off distance, 145 kN/m² of gas pressure and 90° of angle of jet to surface. The results show that a low cost method can be used to measure the absolute signal (sensitivities) of any AE sensors. In addition, Acquaviva et al. (1980) developed the helium gas jet calibration method to describe the variable effects of specimen geometry, couplant and AE sensor characteristics. The result of several experiments on 7039 aluminium show that quantitative agreement can be obtained between laboratories for the spectral shapes and amplitudes of AE emanated during a carefully specified mechanical test.

Prateepasen et al. (2000) applied a calibration procedure using an air jet as the artificial AE source to single-point tool wear monitoring. The calibration procedure involves setting up an air jet at a fixed stand-off distance from the top rake of the tool tip, applying in sequence a set of increasing pressures and measuring the corresponding AE. A tool shank of type SDJCL 1616H 11 and carbide tool inserts of type CG 4035 DCMT 11 T3 04-UF (Sandvik Coromant) are used. Two AE sensors are mounted on the tool-holder: a WD sensor (from Physical Acoustics Corporation: PAC) at the end of the tool-holder and an R30 sensor (PAC) on the side. Then, the ratios of AE spectra of the air jet and tool wear are computed and compared, respectively. From the results, the root-mean-square value of the AE (AE_{rms}) obtained is linearly proportional to the pressure applied. The frequency spectra of the AE produced by the air jet and tool wear are very similar to each other. The frequency response function of the tool/sensor system is purely a function of the frequency and is independent of the input states or input mechanisms such as produced by air pressure or tool wear. It is possible to convert an AE_{rms} value into an equivalent air jet pressure value. The results are concluded that it will be possible to make comparison between results obtained from different set-ups.

2.2.3 Pulsed Laser System Calibration

Clough (1987) reported the energetic of AE source characterization. An AE system is modeled as a linear power flow process. The technique is not limited to large bodies (with diffuse wave fields) because it assumes only linear power flow between source and sensor. The entire AE system (source, specimen, sensor, and instrumentation) is calibrated by use of an energy source such as a dropped ball or pulsed laser. The source strength may then be estimated to an order of magnitude in terms of joules or watts. Over the 63-200 kHz band-pass, the system is linear in power; for the larger bodies (as a

special case), the AE energy is found to be approximately independent of specimen size and shape, as well as source and sensor positions. From the results, the technique can be applied in materials processing, structural monitoring, and materials science studies.

Yan and Jones (2000) outlined and presented a way of calibrating AE sensor systems in situ using a pulsed laser induced AE energy source for calibration of AE sensor and a bouncing ball generated AE energy source for simulation of AE source. Two AE sensors (different sensitivities) are used in the experiment. The calibration tests by a pulsed laser are performed on a 6 mm thick aluminium flat plate of dimensions 214 mm × 161 mm, supported at the corners by four 20 mm thick 18 mm × 14 mm small rubber blocks. The simulation of AE source using a bouncing ball is simulated. The result shows that the laser-calibrated AE sensor systems give good estimations of the AE energy resulting from the bouncing-ball impact standard AE source. More importantly, through absolute energy calibration of the AE sensor systems, not only can the AE measurements be made quantitative, but also the measurements taken by different experiment layouts can be made comparable.

Jones and Yan (2005) presented a possible hierarchy of traceability for AE energy measurements through in situ calibration of the AE sensors using a thermo-elastic pulsed laser irradiation in tool wear monitoring. Two AE sensors (different sensitivities) are used to monitor the tool wear. The machining tests are conducted in a CNC lathe by turning En24T steel and are confined to finishing operations under various cutting conditions set within the tool insert manufacturer's recommendations. The AE sensors are calibrated in situ on the tool by a pulsed laser induced AE energy source. The results show that there is good agreement (average variation within $\pm 3.5\%$) between the AE source energy measurements taken from the two AE sensors, even though there are different sensor locations and different sensitivities. This indicates that the AE sensors calibrated in situ, reliable quantitative AE measurement can be obtained.

2.2.4 Dropping ball

Raeymaekers and Talke (2006) studied the use of AE for detection of tape edge contact using ball drop method for calibration AE testing system. A steel ball is dropped from different heights on a load cell that measures the impact force during contact. Next, a steel ball is dropped from varying heights on the AE sensor and the maximum output voltage is measured. A small tube is used to guide the ball, to insure that the impact of the steel ball occurs at the same position for all experiments. The relationship between AE voltage and impact force from load cell is established. After calibration, the AE testing system is applied to detect the tape edge contact. The results show that the ball drop method can be employed to calibrate the AE testing system for detection of tape edge contact. Furthermore, it is also shown that the maximum of impact force between the flange of a roller and a tape edge was observed to occur for a half full tape reel. The magnitude of the impact force increases for increasing tape speed.

2.2.5 Electrically Driven Ultrasonic Transducer

Yuki and Homma (1996) studied the estimation of AE source waveform of fracture using a neural network. The simulated AE waveform is generated by applying a step voltage (13.8 V) to PZT transducer that is attached to the plate with high vacuum sealing compounds by spring force. An aluminium alloy plate (502 × 403 × 60 mm) taken as a semi-infinite plate is used for the propagation medium of AE wave. AE waveforms are detected by a capacitive displacement sensor (6 mm of diameter) located

on the epicenter (opposite side). From the experimental results, the simulated AE source using a PZT transducer is suitable for providing the learning waveforms since the shape of the source waveform is similar to that of mode I crack extension, and that the rise-time of the source waveform can be controlled by its resonance frequency. It is demonstrated that the appropriate source waveform associated with mode I crack extension is successfully determined by the three-layer network taught with the simulated sources. It is concluded that the AE source waveform analysis using a neural network is effective for the AE associated with mode I crack extension.

Evans et al. (2000) investigated the use of conical PZT transducers as point AE sources. The transducers based on a design originally developed at the National Institute for Standards and Technology in the USA can be used as point transmitters over the frequency range of interest in AE measurements (100 kHz to around 1 MHz). The conical tip is machined from a 10 mm diameter, 3 mm thick PZT disc and has a tip diameter of 1 mm. A 50 μm thick brass is bonded to the tip with conducting epoxy and served as a wear plate and electrical contact. The backing material is made from tungsten associated with epoxy. The backing material assembly is mounted in an aluminium case. From the experiment results, the conical PZT transducer is suitable for use in experiments to calibrate structures so that AE source strengths can be determined. It is also shown that measurements of the response of the transmitting transducer backing can be used to assess the coupling efficiency, and hence to remove concerns about inconsistent coupling affecting the calibration measurements. The results indicate that the variation of the backing response with coupling is due to a shift in the resonance frequencies of the transducer with the mechanical load impedance. In addition, Yan et al. (2002) developed and applied the conical PZT transducer on a 6 mm thick stainless steel flat plate of dimensions 300 mm \times 200 mm, supported at the corners by four 6 mm thick 50 mm \times 50 mm rubber pads. The plate represents a typical geometry of the structures for AE applications. The results show that the conical PZT transducer is a good transmitter for artificial AE source generation. It is also shown that measurements of the response of the transmitting transducer backing can be used to assess the transducer coupling efficiency to the structure. The conical PZT transducer can be used as an absolute simulated AE energy source. It will need to be calibrated against a primary or secondary simulated AE standard energy source such as an elastic ball impact or a thermo-elastic laser-irradiation (Yan et al., 2004).

Theobald et al. (2001) proposed a technique that aims to make the calibration of AE measurements possible with the use of a reference source. The reference sources discussed are a conical shaped PZT transducer with a point contact tip and an elastic ball impact. The ball impact is a source where the stress wave energy produced from the impact can be predicted from the potential energy loss that occurs in the impact. The calibration tests are performed on a 6 mm thick stainless steel flat plate of dimensions 300 mm \times 200 mm, with its surface polished smooth. The conical PZT transducer is used to capture the acoustic wave. The results show the linearity of the both source. The output AE signal energy is in direct proportion to the input AE energy. The proportional constant is dependent on a number of factors including coupling efficiency of the source and sensor, the attenuation or the source and sensor distance, and also on the damping of the plate. Furthermore, it is also shown that a quantifiable primary source such as the elastic ball impact can be used to calibrate a reference source. Such practical calibrated AE source that can be applied in industry would allow for a robust calibration of AE

measurement equipment in situ, thus making quantifiable or traceable measurements of AE possible.

Theobald (2004) and Theobald et al. (2005) reviewed and developed a facility for traceable out-of-plane displacement calibration of AE sensor. The key issues surrounding the development of such a facility are reviewed, including the need to establish repeatable AE sources, select suitable test blocks and to understand the limitations imposed by AE sensors themselves. The laser interferometer is employed to provide an absolute measurement of the displacement on the surface of a test block. The test block is made of Schott NBK7 optical quality borosilicate glass of approximate dimensions 240 mm by 250 mm by 160 mm, and is polished and coated. Thin-film coating of the block with aluminium is performed on the sensor side only, to provide a reflective surface for the laser interferometer, exceeding 85% reflectivity. The tone-burst used for the sensor calibration is produced using a PZT transducer driven by a function generator. From the results, a narrow band, tone-burst technique is demonstrated for the absolute magnitude calibration of AE sensors for the response to compression waves normal to the contacting face. The sensitivity using this method can be derived for a sensor combined with its intended cables, preamplifier and filter unit. This experimental results show an example of one such combination, with a typical peak-sensitivity of 0.27 V/pm. The tone-burst approach is more suited to sensors that are specifically designed to be used at or close to resonance than the impulse response method and allows a good representation of the performance of AE sensor at discrete frequencies across its bandwidth.

Theobald (2009) proposed an optical calibration for both the out-of-plane and in-plane displacement sensitivity of AE sensors. A laser homodyne interferometer is used to measure the out-of-plane and in-plane displacement of the surface of a large test block excited by a repeatable source transducer. A 410 mm diameter hemi-spherical aluminium block with a flat top of diameter 50 mm for mounting the sensor under test is used for the out-of-plane calibration. For the in-plane calibration, a 250 mm diameter hemi-spherical aluminium block with a step machined across the flat top with the vertical face of the 0.5 mm step being optically polished is used. The results show the sensitivity of the sensor to both planes of displacement in the absence of the sensor and show that the two sensors tested are around 10 times more sensitive to the out-of-plane displacement than the in-plane displacement. Since the most AE sensors are designed to work in thickness mode, it is reasonable for the sensor to have in-plane displacement sensitivity much lower than that for out-of-plane displacement. Finally, the use of a laser interferometer as the reference sensor for broadband calibration provides traceability to the wavelength of light, providing a more direct calibration than for reciprocity (Theobald and Pocklington, 2010).

2.2.6 The Method for Analysis the Output Voltage of AE Sensor

Bolin (1979) presented a model for calculating AE amplitudes. The Gaussian distribution function is chosen to describe the transfer function for calculating AE amplitudes. The model is based on a method of describing the stress waves from a local change of an inelastic strain. An ultrasonic calibration is used to test the model. The results show a possibility to correlate the measured AE amplitude with the magnitude of the physical event within the material.



Yarovikov and Bazhenov (1998) presented the analysis of PZT ultrasonic receivers based on the equations of electro-elasticity when the sensitive element is in a state of bulk stress. The theory of wave processes in PZT material and equivalent circuit of a PZT sensor are described. The equations of electro-elasticity are derived and the analogies between electrical and mechanical systems are explained. The result shows that the simplified formulas (derived from the theory) can be used to calculate the amplitude (voltage) characteristics of AE sensor, based on a ring PZT element.

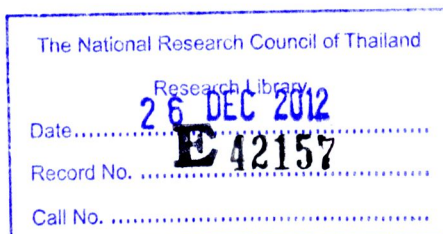
Sherrit et al. (1999) presented the comparison of the Mason's and KLM equivalent circuits for PZT resonators in the thickness mode. The parameters of the KLM and Mason's equivalent circuits in the thickness mode are presented for the case where dielectric, elastic and PZT losses are present. The models are compared. From the experimental results, the models are found to be equivalent under a variety of boundary conditions when the loss is applied consistently in each of the models. The effect of PZT, dielectric and elastic loss coefficients on the overall shape of the insertion loss curve is found to be small and independent of the designation of PZT loss. The dissipated power in the transducer is found to be dependent on the PZT loss designation, which suggested that the PZT loss is important for determining heating effects in the transducer.

2.2.7 Transfer Function between AE Sensors

Prateepasen and Srinang (2008) presented an AE transferability method in applications of internal valve leakage rate measurement and tool wear monitoring. The method aims to transfer the information between AE measurement systems using different types of AE sensor and position by relationship that is called a transfer function. The spectrum density function/AErms spectra of both wide band (WD) and resonance (R15 and R30) AE sensors are studied. A tool shank and carbide tool inserts are used. Two AE sensors are mounted on the tool-holder (a WD sensor at the end of the tool-holder and an R30 sensor on the side). Three sets of cutting condition of tool wear monitoring in machining tests are conducted. For internal valve leakage rate measurement, artificial leaks from incomplete closure of ball valve are used to simulate the leakage. The tests are conducted by varying inlet pressure from 1 to 5 bars in three valve sizes of 1, 2 and 3 inches respectively. The AE signals detected at the two sensors (WD and R15) are analyzed. Transfer functions of two AE sensors are calculated and represented by the ratio of frequency responses of the two sensors. The results show a very good similarity transfer function in various conditions. This is particularly useful since the information obtained from one sensor may be converted into another without having to repeat the experiments. With the proposed acoustic transferability, it will be possible to make comparison between results obtained from different set-ups.

2.3 Internal Valve Leakage Rate Measurement Using AE

Sharif and Grosvenor (1998) studied the internal valve leakage detection using an AE measurement system. The aim of authors is to determine the lowest detectable compressed air leakage rate through an industrial control valve that can be reliably detected using AE technique. Through-valve leakage is deliberately introduced into a 25.4 mm hard-seat globe type control valve under controlled conditions. Two AE sensors together with the AE data acquisition and processing systems are used to monitor a wide range of leakage rates under different working conditions. The effects of the background noise on the measured AE signal are considerably reduced by using the real-time programmable filters that are part of the AE measurement system. The results



show that a very low leakage rate, less than 0.2 l/min, at a differential pressure as low as 110.3 kPa can be reliably detected by AE in an industrial environment. This leads to an acknowledgement that the AE technique is suitable for detecting very low leakage rate at sure a low differential pressure and in industrial environments. It can also be concluded that the AE leak detection techniques provide more reliable and consistent results in industrial applications in comparison with the vibration analysis method. This is due to the high level of background noise that is usually present in an industrial environment and when the vibration method is used, the background noise produces considerable interference with the leak-related frequency components. AE, on the other hand, operates at frequencies that are well beyond the frequency range of the mechanical noise. Finally, the result is demonstrated that although the resonant AE sensor with the frequency response in the range 20-100 kHz more sensitive for the detection of lower leakage rates (less 0.2 l/min at 110.3 kPa), for industrial applications the sensor with the higher frequency response (0.1-1 MHz) is more suitable in order to reduce the need for noise reduction filtering to a minimum level.

Lee et al. (2003) demonstrated the capability of each sensor including AE, accelerometer, and ultrasonic (UT) to provide diagnostic information useful in determining check valve aging and service wear effects, check valve failures, and undesirable operating modes. In this study, as the first step, an application of AE sensor and accelerometer for on-line monitoring of condition of check valve is studied. From the experimental results, the AE sensor and accelerometer can be used effectively for condition monitoring of leak test of check valve. It is demonstrated that the characteristic of leak signals obtained from both AE sensor and accelerometer indicates higher increase of voltage in waveform and rapid decrease of amplitude in FFT spectrum. In addition, the UT sensor provided useful tool for detection of disk of check valve. This study is developed advanced sophisticated signal processing, noise reduction, and pattern recognition techniques and algorithms from check valve degradation.

Lee et al. (2004) presented the analysis of AE signals for condition monitoring of check valve in nuclear power plants. The aim of authors is to identify and recommend methods of inspection, surveillance, and monitoring that would provide timely detection of valve degradation and service wear so that maintenance or replacement could be performed prior to loss of safety functions. The AE technique is used to provide diagnostic information on the determination of check valve aging and degradation, check valve failures and undesirable operating modes. In this study, AE signals due to leak from check valve with artificially leakage and artificially worn disk are studied both analytically and experimentally. The results show that the AE technique can be employed to monitor the check valve in nuclear power plants.

Kaewwaewnoi et al. (2005) presented a method to measure leakage rate of gas through valve using AE technique. Three sizes of the ball valve that are 1, 2 and 3 inches in diameter are used. Air from an air compressor and controlled by a regulator is selected to used instead of gas. The valve inlet pressure is varied from 1 to 5 bars with an increment of 2 bars. An AE sensor (resonant frequency of 150 kHz) is mounted on the case of the valve to capture the AE signal since its frequency response covered the frequency range of the leakage. From the results, it is found that the AE activities increased with the leakage rate, the inlet pressure but diminished with the valve size. An expression to explain the relationship between these parameters is also introduced in

this work. Finally, it can be concluded that the AE technique can be used to detect valve leakage at high sensitivity.

Chen et al. (2005) studied experimentally AE to monitor internal leakage in modern water hydraulic cylinders. For the experimental setup, a modern water hydraulic system and an AE measurement system were used. The water hydraulic system includes a PPH 12.5 (trade name) water hydraulic power pack and an AQUA70 (trade name) water hydraulic cylinder. The cylinder has a piston diameter of 50 mm and a stroke of 500 mm. A broad band AE sensor (WD) is used to measure AE signals. Through these experiments, the background noise induced by the operation of a water hydraulic system is carefully determined, AE signals generated by a water hydraulic cylinder operating under different piston-sealing conditions are characterized, and AE signals generated by internal leakage in a water hydraulic cylinder are also characterized. The measured AE signals are analyzed using the power spectral density technique. From the experimental results, AE technique is not affected by background noise of a water hydraulic system. In this study, the detected background noise is very weak and does not interfere with the high-frequency AE signals of interest. AE technique is sensitive to internal leakage in a water hydraulic cylinder. It is found that the internal leakage through the clearance between the piston and the cylinder bore generated significant AE signals at a certain frequency. Furthermore, the AE amplitude of the dominant peak increased as the leakage rate increased. This AE amplitude may be used as an effective internal-leakage-related feature for condition monitoring. The results show that AE may be used to develop an effective technique for condition monitoring of internal leakage in modern water hydraulic cylinders. However, this research only conducted a qualitative investigation of the problem.

Lee et al. (2006) studied the detection of internal valve leakage using AE method. The aim of this study is to estimate the feasibility of AE method for the internal valve leakage. Two types of valve (a 4 inch globe steam valve and 4 inch ball water valve) leak tests using three different leak paths and various leak rates are preformed in order to analyze AE properties when leaks arise in valve seat. Two AE sensors (narrow frequency band) were used in this study. The test system is supplied with saturated steam at a nominal pressure of 600 psi. As a result of leak test for specimens simulated valve seat, it is confirmed that leak sound amplitude increased in proportion to the increase of leak rate, and leak rates are plotted versus peak AE amplitudes. The resulting plots of leak rate versus peak AE amplitude are the primary basis for determining the feasibility of quantifying leak acoustically. The large amount of data attained also allowed a favorable investigation of the effects of different leak paths, leak rates, pressure differentials and AE sensors on the AE amplitude spectrum. From the results, it is suggested that the AE method for monitoring of leak is feasible.

Lee et al. (2006) demonstrated the characteristics of the AE signals for condition monitoring of check valves in nuclear power plants. The aim of authors is to investigate the advanced condition monitoring systems, based on the AE method, which can provide timely detection of check valve failures. AE testing for a check valve under controlled flow loop conditions is performed to detect and valve degradation such as wear and leakage due to foreign object interference. Although much of the work described is made to demonstrate feasibility of the specific approach, the results are promising and indicate that AE techniques have the potential to predict accurately from flow characteristics and the behavior of check valve leakage such as disc wear and

foreign object failures. In addition, it is found that the frequency spectrum would be capable of directly detecting a 150 kHz frequency acoustic wave generated from the backward leakage flow. And also, the frequency spectrum profiles of the check valve leakage do not depend on the leak rate and the pressure, but that they are strongly dependent on the types of the failure modes. The neural network algorithm for identifying failure modes and estimating the failure sizes in a check valves is also developed by Lee et al. (2005). The neural network algorithm shows a good solution for detecting and identifying a failed check valves.

Kaewwaewnoi et al. (2007) presented a novel method to make the ratio of AE_{rms} spectra of AE sensors in the application of valve leakage rate detection. This method aims at transferring the information between AE inspection systems using different types of AE sensor by relationship called a transfer function. The spectrum density function / AE_{rms} spectra of both wide band and resonance AE sensors are studied. In this experiment, artificial leaks from incomplete closure of ball valve are used to simulate the leakage. The tests are conducted by varying inlet pressure from 1 to 5 bars in three valve sizes of 1, 2 and 3 inches, respectively. The results demonstrated that the response ratio of the sensors may only be valid in the overlapping pass band of both sensors due to inherit numerical instability of the ratio computation. Nevertheless, the result is still practically useful with the application of AE_{rms} instead of individual frequencies of the whole spectrum.

Chen et al. (2007) analysed the characteristics of AE signals generated by internal leakage in a water hydraulic cylinder. Experiments are carefully designed, including the simulation of the internal leakage across the piston seals in a water hydraulic cylinder and the measurement of the internal leakage rate. AE signals obtained from the experiments are analysed, in which several AE parameters are extracted from the AE signals and the effectiveness for predicting the internal leakage rate are studied. From the experimental results, AE signals are sensitive to small internal leakage in a water hydraulic cylinder and AE-based methods are able to predict the internal leakage that is smaller than 1.0 L/min. Energy-based AE parameters, whether measured in the time domain or in the frequency domain, are more suitable than the AE count rate and the peak power spectral density magnitude to interpret AE signals generated by the internal leakage. The AE_{rms} value has a strong linear relationship with the internal leakage rate in a water hydraulic cylinder, and therefore, it is a most desirable parameter for describing AE signals in the development of a quantitative AE model to determine the internal leakage rate.

Kaewwaewnoi et al. (2010) presented a theoretical investigation of the AE to detect the internal leakage rate through a valve and experimental validation. The AE signals generated by internal liquid and gas leakage through valves are characterized. The effect of the influenced factors of leakage rates, inlet pressure levels, valve sizes and valve types, on AE parameter, AE_{rms} , are studied and explained. Two types of ball and globe valves are used in the experiment (25.4, 50.8 and 76.2 mm of inside diameters). For liquid leakage, the leakage ranged from 1.0 – 6.0 l/min due to incomplete closure is selected to study. A piston pump is used to generate water flow with the inlet pressure maintained between 100 and 700 kPa. For gas leakage, air from an air compressor and controlled by a regulator is selected to used instead of gas. From the results, it is confirmed that the sound power theoretically derived was in good agreement with the AE signal power. This parameter extracted during water valve leakage can be used to

predict the actual leakage rate qualitatively. The effects of inlet pressure, leakage rate, valve size and valve type on AE_{rms} are determined. In addition, it is found that the characteristics of the AE signals generated by internal valve leakages of both compressed air and water are different. The investigation relationship is easy to implement and its benefits are reducing the amount of experiment data necessary and utilization for a knowledge base for a new AE instrument.

2.4 Monitoring of Corrosion Process Using AE

Kudryavtsev et al. (1981) reported the detection of hydrogen embrittlement of carbon steel using AE. The Ck 35 steel was used in this experiment by electrochemically charged with hydrogen. The testing material was electrodeposited by cadmium. AE analyses are correlated with the conditions of hydrogen charging and the analytically measured hydrogen content. A correlation between the signals of AE and the embrittlement of the material is loaded up to the yield strength, unloaded, and reloaded again. From the experiment results, materials without hydrogen embrittlement show AE signal in the second load phase only if the level of the first load is exceeded. However, hydrogen embrittled material shows AE signal in the second load phase even beneath the level of the first load phase. It is concluded that the AE technique can be employed to detect the hydrogen embrittlement of carbon steel.

Weng et al. (1982) reported a nondestructive monitoring technique to detect, characterize, and locate corrosion induced structural damage and presented the AE characterization of corrosion induced damage in reinforced concrete. AE technology is used to monitor and characterize the deterioration process in a series of controlled laboratory tests. Three groups of experiments were performed. The first involved polarization scans upon reinforcing steel, the second addressed accelerated corrosion tests upon reinforced concrete specimens and the third involved potential monitoring of naturally corroding reinforced concrete specimens. By comparing measured AE characteristics, including counts and amplitude distributions, with physical examination of test specimens at various phases of corrosion induced damage, a relation between the observed damage and the attendant AE is developed (Dunn et al., 1984). The results demonstrated that measurable levels of AE occur even under freely corroding exposure of reinforced concrete. It is concluded that AE monitoring may represent a useful technique for corrosion damage characterization of reinforced concrete.

Hill et al. (1989) outlined and presented the detection of stress corrosion cracking (SCC) in an E-glass chopped strand mat-reinforced polyester resin using AE. AE activity is observed when samples under tension, having exposed cut edges, are subjected to an environment of either sulphuric acid. In water there is negligible AE, showing that the acid corrosion AE originates from chemical attack rather than merely physical penetration of aqueous solution. Linear location of AE signals proves to be an efficient means of determining the onset of SCC in acid, while the AE amplitude distribution is also useful in this respect. From the experimental results, AE is a useful method for monitoring and locating stress corrosion damage in real time in composite material. In tensile specimens, linear location of the AE is particularly effective for determining the onset and position of SCC, which form spontaneously in the material in sulphuric acid. The AE amplitude distribution can also be used as an indicator of the presence of SCC. The AE event count gives an approximately linear measure of the residual strength. It is concluded that the cumulative AE event count is approximately proportional to the crack area.

Jones et al. (1991) studied the evaluation of stress corrosion crack initiation using AE technique. The AE technique was used to detect the development of short inter-granular stress corrosion cracks in laboratory samples of sensitized type 304 (UNS S30400) austenitic stainless steel. Tests are conducted at 25°C in water containing either 15 ppm of Na₂S₂O₃ or 100 ppm of NaCl. Cylindrical samples with PZT sensors mounted on both ends and the corrosion cell confined to the gauge section are used. The dual PZT sensors allowed discrimination between signals generated within the sample from those generated from the surroundings. The experiment results show that inter-granular stress corrosion cracks of 200 to 300 µm length by 100 to 200 µm depth can be reliably detected with this technique. Shallow 10-µm-deep longitudinal flaws are also detected in tests conducted in the 100 ppm NaCl environment.

Seah et al. (1993) reported the correlation between AE signal and corrosion rate. The mild steel (AISI 1020) of size 50 mm long, 25 mm wide and 3 mm thick was used for experiment. A resonance PZT sensor, bandwidth of 100-300 kHz, was selected to monitor the corrosion process. The method used for monitoring the AE signal is count (ring-down counting). The experiment result shows that there is a marked correlation between AE activities and corrosion rate. The mean amplitudes of the AE signals due to corrosion are well above the ambient noise level and this enables the AE signal to be detected easily. It is also possible to detect the different stages of corrosion, namely uniform corrosion, non-uniform corrosion and intense localized corrosion in naturally aerated acid solution, based on the observed AE count rate. The method may also be useful for the detection of hydrogen bubbles as a by-product of corrosion.

Ferrer et al. (1999) studied the monitoring of abrasion corrosion of austenitic stainless steel (AISI 304L) in saline solution using AE technique. The abrasion mechanism is first examined for three angles (30, 45 and 90°) of impingement in non-corrosive conditions. A potentiostat is used to control the electrochemical corrosion process. The sensors are wideband (80 kHz–1MHz) type PZT ceramic. The abrasive particles are SiC particles (average grain size: 125 µm). Then, the synergistic effect between mechanical damage and corrosion was investigated. The experimental results indicate that the lower the impingement angle, the lower is the mechanical contribution. In corrosive conditions, it is shown that, at low abrasion rate, the synergistic effect depends on the impingement angle. Some hypothesis are proposed in order to separate, in the overall synergistic damage, the effect of abrasion on corrosion and the effect of corrosion on abrasion (Ferrer et al.,2000). In the experimental results, the AE technique can be employed to monitor the abrasion corrosion of austenitic stainless steel. In multi-impact conditions, it is shown that acoustic energy can be taken as reference in order to quantify not only the overall energy of the impacts but also the mechanical damaging. Simultaneous time analyses of corrosion potential and acoustic energy are performed and a good correlation of the instantaneous variations of these parameters is evidenced.

Bellenger et al. (2002) studied the early detection of aluminum alloys exfoliation corrosion using AE technique. The aim of authors is to use the AE technique for detection and monitoring the localization of pitting corrosion on aluminum alloy. The experiment is conducted on two aluminum alloy (Al 2024 T3, and Al 7449 T6 and T7). Samples are immersed 4 days in the modified ASTM STP 1134 saline solution. From the experimental results, the exfoliation corrosion sensitivity of alloy 7449 T6 is more important than for alloy T7 that exhibits only the presence of small and non-occluded pits. Very severe exfoliation corrosion is also observed on Al 2024 T3, but after a

longer immersion time or in a more acid solution. In the results, the recording of the AE activity shows evident links between this activity and the exfoliation corrosion rate. The analysis of the characteristics of signal reveals a population corresponding to the release of hydrogen bubbles. A few more energetic signals have also been observed. The source can be either, the cracking resulting from the separation of sheets of metal, or the development and evolution of hydrogen bubble formed inside blisters during exfoliation corrosion.

Saenkhum et al. (2003) studied the classification of corrosion severity detected by AE. The AE signals are analyzed to reveal the correlation between AE parameters and severity levels of pitting corrosion in austenitic stainless steel 304 (SS304). In this research, the corrosion severity is graded roughly into five levels based on the depth of corrosion. Relationships between a number of time-domain AE parameters and the corrosion severity are first studied and key parameters identified. The corrosion severity is also categorized into three stages: initial, propagation and final stages based on the source mechanisms of the AE signals. Authors identified these stages from the frequency-domain characteristic of the AE signal and the visual characteristic of the corroded pits in each level of corrosion severity. A number of measures are employed to quantify such characteristics and the source mechanisms hypothesized. To demonstrate the usefulness of such parameters, a feed-forward neural network is used to classify the corrosion severity. Preprocessing and verification techniques are provided to facilitate and to maintain the generalization capability of the network. From the experimental result, the classification performance is excellent and demonstrates that the AE technique and a neural network can be efficiently used to detect and monitor the occurrence of corrosion as well as to classify the corrosion severity.

Jomdecha et al. (2004) presented a novel low-cost AE source-location system to locate corrosion sources in AISI304 austenitic stainless steel. Four types of corrosion: uniform, pitting, crevice and stress corrosion cracking (SCC) (Jomdecha et al., 2007) are experimented and analyzed. The thickness of each specimen is 1 mm. For uniform corrosion, a corrosive environment is 30% NaCl solution with pH of one controlled by HCL hydrogen bubble nucleation acceleration. For pitting and crevice corrosion, an electrochemical environment is organized using 3% NaCl solution with pH of two controlled by HCL and a potentiostat. For SCC, stress corrosion on a three-point loading bent beam is utilized to produce tensile stress on the specimen according to the ASTM G 39-90 Standard. The specimen is dipped into the 3% NaCl electrochemical solution with pH 2. A Field Programmable Gate Array (FPGA) is employed as the main part in the front-end electronics to compute the arrival-time differences and to transmit the result to a PC via a serial communication. The data are analyzed and then presented in the PC. Three AE sensors with 150 kHz resonance frequency are used to detect the AE activities generated from the corrosion. From the experimental results, the uniform corrosion can be located more accurately than those from pitting and crevice by detecting AE from the hydrogen bubble nucleation of passive film in stable state. However, detecting AE from pitting corrosion source in stable state can not be located correctly. For SCC, the SCC is produced at the midpoint of the specimen dipped into the electrochemical environment. As results, the proposed AE source location system is able to locate corrosion by detecting AE source generated mainly from hydrogen bubbles of AISI304 austenitic stainless steel.

Assouli et al. (2005) studied the detection and identification of concrete cracking during corrosion of reinforced concrete by AE coupled to the electrochemical techniques (potentiodynamic and electrochemical impedance spectroscopy: EIS). The objective of authors is to study the effect of chloride ions on passivity breakdown of steel, in simulated concrete pore solution (SCP) and in concrete reinforcement, and to reproduce the carbonation phenomena by applying to the concrete samples a heating-cooling cycles. The electrochemical measurements are carried out on E24 steels. The wide band PZT sensor (WD) was applied in this experiment. The experimental results show that the carbonation process is very aggressive with chloride ions and show a perfect correlation with AE evolution. A physical model of the reinforcement/electrolyte interface is proposed to describe the behavior of the reinforcement against corrosion in chloride solution. It is concluded that the AE technique can be employed to detect and identify the concrete cracking during corrosion of reinforced concrete by coupled to the electrochemical technique.

Jirarungsatian et al. (2005) reported and studied the monitoring of pitting corrosion in stainless steels using AE. A correlation between AE activity and pitting corrosion is studied. AISI 304 and AISI 316L austenitic stainless steels generally used for storage tank are selected as the specimens in this study. To accelerate the corrosion rate, the electrochemical process is applied. A potentiostat is used to control the electrochemical corrosion process. The progression of the pitting corrosion is measured by a Scanning Electron Microscope and optical microscopy. From the experimental results, the corrosion stage of both types of stainless steel can be divided into two groups: the breakage of the passive film and the progress of the corrosion. The frequency domain responses of AE signal obtained from corrosion process of different types of stainless steel are dissimilar whereas those of the same type are alike. Count, rise time, amplitude, energy and duration time are chosen as the classification features for a Probabilistic Neural Network to classify the corrosion severity into one of five classes. The performance of the network is high. The number of correct prediction is higher than 92% for all classes of corrosion severity.

Ing et al. (2005) studied the cover zone properties influencing AE due to corrosion. The research presented investigates the potential of AE as a means of identifying corrosion at an early stage, before any significant cover damage has occurred. The purpose of authors is to identify the influential cover zone factors that affect the magnitude of the AE measurements per gram of steel loss. Prisms with various combinations of strength, cover thickness, aggregate and rebar diameters are studied to ascertain the important variables likely to be encountered on reinforced structures. The experimental results show that early corrosion, verified by internal visual inspection and mass loss, can be detected by AE technique and before any external signs of cracking. They also show that the most influential parameter affecting the AE measurement is concrete strength, being exponentially related to the AE energy. Material properties, such as cover thickness, had a negligible effect on AE energy during the initial stages of reinforcement corrosion, whereas from this initial work, the rebar diameter indicated a promising relationship with AE energy per gram of steel loss.

Prateepasen et al. (2006) demonstrated the identification of AE source in corrosion process and discussed the effect of the different corrosive condition on AE source. The evaluation of corrosion mechanism is explained that the corrosive mechanism by AE parameters is corresponding to the characteristic and acoustic source of the corrosion

process. In each corrosive stage, the theoretical explanation and observation are used to investigate a physical changing due to corrosion. The AISI 304 austenitic stainless steel was selected as the specimens in this study. A potentiostat was used to control the electrochemical corrosion process. Two tests were conducted at room temperature using an acidic 30% chloride solution in passive tests procedure and 3% NaCl solution in electrochemical process. The experimental results show that different corrosive environment condition causes different dominate AE source. In high concentration chloride test, impact and burst of hydrogen bubble is dominated whereas in electrochemical corrosive test, the AE sources are passive film breakage and pitting corrosion. AE parameters exhibit good correlation with corrosion activities. In high corrosion chloride test, AE signal in frequency domain displays high relationship with size of the bubble. For electrochemical corrosive tests, the number of AE hit is high at the initial stage and significantly decreases in the pitting corrosion stage. The frequency spectrums of AE signal are identical for both stages.

Prateepasen et al. (2006) studied the effect of sulfuric acid (H_2SO_4) concentration on AE signals in uniform corrosion process. The mild steel (ASTM A36) was selected as the specimens to study the characteristic of AE signals received from the uniform corrosion mechanism in various concentrations of H_2SO_4 solution (4.5, 5, 5.5, 6.0 and 6.5 of pH, respectively). The range of pH refers to the pH value range in the crude oil. The potentiostat was used to control the electrochemical of corrosion process at the static corrosive potential (E_{corr}). AE signals are captured using a resonant sensor (R15). From the experimental results, the investigation of scatter plot of AE parameter as Duration-Counts and Duration-AE Energy can explain the corrosion mechanism that released acoustic signals with different characteristics. The AE analyzes shows that the difference of pH values has more influence to corrosion rate than the sulfur atom concentration in H_2SO_4 solution. The cumulate hits and amplitude of detected AE signals can describe corrosion rate. The emissive source of corrosion process in this work is believed to be the breakage of passive film and the uniform corrosion formation. Although other emissive sounds can be detected by AE sensor such as the friction phenomenon of the H_2 bubbles on the material surface or the electrical noise but they are eliminated by frequency filter, threshold sets of noise and experiment set up. And the no bubble in second experiment can explain and confirm that the bubble activity does not effect to corrosion monitoring by AE technique. This work studied the effect of difference in sulfuric acid concentration in crude oil by AE evaluation and can be explained when AE technique is applied to corrosion monitoring in field.

Shaikh et al. (2007) reported the evaluation of stress corrosion cracking (SCC) phenomenon in an AISI type 316LN stainless steel using AE technique. The compact tension specimens, fabricated as per ASTM E399, are polished to 600 grit finish and then graduated on the surface with lines 0.5 mm apart. The stress intensity factor (K_I) for pre-cracking is decreased from 25 $MPa\ m^{0.5}$ to 18 $MPa\ m^{0.5}$ with increasing pre-crack length. The pre-crack length is about 2 mm. These specimens are then subjected to SCC testing in 45% magnesium chloride solution at 413 K in the range of stress intensity factors of 13-26 $MPa\ m^{0.5}$ using the constant load testing method. From the experimental results, AE with amplitudes ranging from 27.6 to 46.5 dB with different counts, energy and rise times occurred during SCC. The analysis of the AE signals in conjunction with fractography indicated that a surge in the AE counts and energy indicated initiation of SCC. AE is found to be continuous prior to the initiation. The time gap between AE events increased during initiation. AE events occurred in bursts

during crack growth. Plastic deformation ahead of the crack tip is determined to be the major source of AE during propagation of SCC in type 316LN stainless steel. The cracking is found to initiate and propagate in the trans-granular mode.

Ramadan et al. (2008) studied the stress corrosion cracking (SCC) of high-strength steel used in pre-stressed concrete structures using AE technique. A simulated concrete pore solution at high-alkaline ($\text{pH} \approx 12$) contaminated by sulphate, chloride, and thiocyanate ions is used. This study is carried out on bare eutectoid cold drawn steel (seven-wires strand of 12.5 mm in diameter). The strand consists initially of a steel central straight wire surrounded by six helical wires. Pre-stressing steel has a fine pearlitic and fully oriented microstructure. Four wide band PZT sensors (WD) are employed. The evolution of the AE activity recorded during the tests shows the presence of several stages related respectively to cracks initiation due to the local corrosion imposed by corrosives species, cracks propagation and steel failure. Microscopic examinations pointed out that the wires exhibited a brittle fracture mode. From the results, the cracking is found to propagate in the trans-granular mode. The role of corrosives type and hydrogen in the rupture mechanism of high-strength steel was also investigated. This study shows promising results for a potential use in situ of AE for real-time health monitoring of eutectoid steel cables used in pre-stressed concrete structures.

Kasai et al. (2009) studied the correlation between corrosion rate and AE signal in an acidic environment for mild steel. The mild steel test piece and sulphuric acid solution in SiO_2 grains (from 20 wt.% to 35wt.%) were used in the experiment. The pH of the medium of the SiO_2 and the sulphuric acid solutions was changed from 1 to 4. A potentiostat was used to control the electrochemical corrosion process. The AE sensor of R 15 was selected to monitor the corrosion process. From the experimental result, the AE signal shows good correlation with the corrosion rates of the test pieces. The corrosion behavior of the test pieces is then discussed with the corrosion potential measured during the experiments. Furthermore, the cathode current is changed to control the generated hydrogen gas volume. The volume of the hydrogen gas generated from the cathode reaction is correlated to the AE signals.

Jirarungsatian and Prateepasen (2010) presented an AE parameter as an alternative to AE activity for classification of corrosion sources. Uniform corrosion in mild steel of type ASTM A36 and pitting corrosion in austenitic stainless steel (SS304) were selected to study. A potentiostat was used to control the electrochemical corrosion process at the static corrosive potential. E_{corr} and E_{pit} were determined from the polarization curve for uniform and pitting corrosion, respectively. From the experimental results, the AE sources in uniform corrosion processes can be divided in to two categories, namely, gas bubble and uniform corrosion. The categorization can be determined using the key AE parameters of resonant frequency. For pitting corrosion, the AE sources in the context of pitting corrosion can be classified in to three groups using the selected AE parameters, together with the theory of corrosion mechanisms: (i) gas bubbles by using their resonant frequency, (ii) passive film rupture by using duration time and relating to the initial time of metastable pit formation according to electrochemical analysis, and (iii) pit propagation as related to the time of occurrence and pitting corrosion mechanisms. The benefit of this approach is that one can better classify AE sources. Signals from actual AE sources can be derived and processed. In addition, the resulting information is essential to separate noise from signal in corrosion applications.

